

Direct measurement of bulk currents in the quantum Hall regime

S. Sirt,¹ V. Y. Umansky,² A. Siddiki,³ and S. Ludwig^{1,*}

¹Paul-Drude-Institut für Festkörperelektronik, Leibniz-Institut im

Forschungsverbund Berlin e.V., Hausvogteiplatz 5-7, 10117 Berlin, Germany

²Weizmann Institute of Science, 234 Herzl Street, POB 26, Rehovot 76100, Israel

³Istanbul Atlas University, Hamidiye, Anadolu Cd. no:40, 34408, Istanbul, Turkey

The integer quantum Hall effect can be observed in a two-dimensional conductor penetrated by a perpendicular magnetic field and with edges connecting the current carrying contacts. Its signature is a state of quantized Hall and simultaneously vanishing longitudinal resistances. A widely accepted model is the Landauer-Büttiker picture, which assumes an incompressible, i.e., electrically insulating bulk state surrounded by current carrying one-dimensional edge channels. This single-particle model is challenged by the screening theory. It derives, that electron-electron interaction leads to a fragmentation of the Hall bar into compressible and incompressible strips, where the latter gradually shift from the sample edges into the bulk with increasing magnetic field. This suggests a transition from edge to bulk current if we associate current flow with incompressible strips. We present a direct experimental proof of this transition from edge to bulk current. Our results support the screening theory.

I. INTRODUCTION

Since its discovery in 1980 by Klaus von Klitzing [1], the integer quantum Hall effect (QHE) has been a subject of fundamental research and today provides the recommended standard for calibrating electrical resistance [2, 3]. The QHE is a manifestation of the Landau quantization of the charge carriers density of states (DOS) when exposed to a magnetic field. Its main features are extended plateaus of the Hall resistance as a function of the magnetic field at quantized values $R_V = R_K/\nu$, where $R_K = h/e^2$ is the fundamental von Klitzing constant and the integer filling factor $\nu = 1, 2, 3, \dots$ measures the fraction of occupied Landau levels (LLs). Despite the relative maturity of the QHE, its microscopic nature is still controversially discussed. It goes without saying that the microscopic details are important for both, our fundamental understanding of the QHE and our ability to optimize the accuracy of its metrological application. In particular, the question where the current flows and whether it is free of scattering and entirely coherent is central for possible quantum technology applications, because the phase accumulated by a charge carrier crucially depends on its path way [4, 5]. Further, our model of the integer QHE serves as a basis for understanding its relatives, such as the fractional, spin or anomalous QHEs.

The Landauer-Büttiker (LB) picture [6, 7] considers non-interacting electrons in equilibrium. It predicts for the entire range of the plateaus chiral current flow through ν quasi one-dimensional (1D) edge channels. The bulk of the sample is assumed to be insulating, caused by the Landau gap of the DOS, where the gap is maintained by Anderson localization. Assuming complete suppression of back-scattering inside the chiral edge channels, one then finds that each (spin-resolved) edge channel would carry the quantized conductance of a perfect 1D channel, R_K^{-1} .

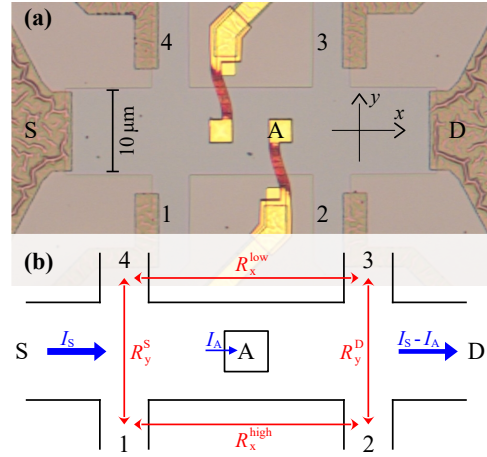


FIG. 1. (a) Microscopic photograph of the sample. The mesa (gray color) shapes the $10\mu\text{m}$ wide Hall bar containing the 2DES at a depth of 130nm . Where it appears brown and smooth, the surface is etched to a depth of $\approx 240\text{nm}$. Dark and rough brown regions indicate the ohmic contacts S, D, 1–4. Bright yellow regions are gold gates with air bridges (red) connecting to two inner ohmic contacts (hidden below the squared $2.5\mu\text{m}$ wide gold regions). The left one is always electrically floated (unused), while contact A is connected to ground in some of our measurements. (b) Sketch showing contacts, imposed current contributions and resistance matrix elements; voltage probes 1–4 are floated.

The screening theory goes beyond the LB picture as it derives the local electrostatic potential landscape in a self-consistent calculation. It takes into account the influence of the direct Coulomb interaction of the charge carriers within the Thomas-Fermi approximation while including the quantum nature of the electrons within a mean field approach. It thereby accounts for the Hall voltage caused by a finite imposed current [8–14]. For the case of equilibrium (zero imposed current), the electrostatics predicted by the screening theory was recently confirmed (for $\nu \leq 3$) by self-consistently solving the full quantum-electrostatic problem

* sirt@pdi-berlin.de; ludwig@pdi-berlin.de

without using the Thomas-Fermi approximation [15].

According to the screening theory, the Landau quantization gives rise to a local bandgap between either completely filled or empty LLs, such that incompressible strips (ICS) emerge, in which electron scattering is completely absent (at low enough temperature). The ICSs separate compressible regions, inside which a LL is partly filled, so that electrons can scatter. The compressible regions are perfectly screened with the LL pinned at the local chemical potential. Therefore, both, the energies of the LLs and the chemical potential vary inside the ICSs only.

Being proportional to the local potential gradient, the current density is non-zero inside the ICSs. An imposed current modifies the electrostatics and the potential drops inside of the ICSs. Considering the situation far from equilibrium (sizable imposed current), clearly suggests that the imposed current flows inside the ICSs, too [16], while the compressible regions remain free of current [9, 14, 17]. Inside the ICSs the Landau gap suppresses scattering, such that the longitudinal resistance vanishes along the Hall bar, while the dissipation happens in the ohmic contacts. Integrating the current density over the ICSs then gives rise to the observed quantized Hall resistance $R_V = R_K/v$. Only, once the imposed current exceeds the breakdown limit of the QHE, the ICSs vanish and the transport becomes diffusive [18–20].

In contrast to LB edge channels, the ICSs are not 1D. Instead the width of an ICS grows as the magnetic field B is increased along the quantized Hall plateau. While growing wider, the ICSs gradually move from the edge towards the center of the Hall bar, where they combine into a single ICS. The exact position and geometry of the ICSs depend on the local electrostatic potential combining the confinement, the Hall potential and the screening via electron-electron interaction. Disorder fluctuations are not directly included in most calculations based on the screening theory. Disorder would counteract the predicted asymmetric development of the ICSs along a quantized plateau. However, in contrast to the LB picture, the screening theory predicts plateaus with finite widths even at zero disorder [21]. In order to experimentally test the screening theory, we keep the influence of disorder small by using a relatively narrow high mobility sample with the mean-free-path exceeding its width, cf. Sec. II.

An increasing number of experiments support the screening theory and thereby provide indirect evidence for the existence of ICSs [22–29]. Magnetic imaging of a quantum anomalous Hall insulator was interpreted in terms of bulk current [30]. In the present article, we go one step further by performing a direct measurement of bulk current while the Hall resistance is quantized. To achieve this, we use an inner ohmic contact placed near the center of our high-mobility Hall bar. Our result exceeds the scope of the LB picture and supports the screening theory.

II. SETUP

Our $10\ \mu\text{m}$ wide Hall bar is carved from a GaAs/AlGaAs heterostructure containing a two-dimensional electron system (2DES) $130\ \text{nm}$ below the surface. We cool it to a temperature of $T \simeq 300\ \text{mK}$ in a He-3 evaporation cryostat. At this cryogenic temperature, the carrier density and mobility of the 2DES are $n_s \simeq 1.2 \times 10^{11}\ \text{cm}^{-2}$ and $\mu \simeq 4 \times 10^6\ \text{cm}^2/\text{Vs}$, respectively, as determined from our Hall measurements. (The corresponding mean-free-path, $\lambda_m \simeq 23\ \mu\text{m}$, exceeds the Hall bar width.) In Fig. 1(a), we present a micrograph of the Hall bar. It contains two small ohmic contacts close to its center. For this article, the left one is always electrically floated and does not affect the measurements, while in some measurements we connect the contact labeled A to electrical ground.

To perform direct current measurements (using a Keithley 2450 sourcemeter), we impose a constant current $I_S = -100\ \text{nA}$ (corresponding to $V_S < 0$) through the source contact S, while the drain contact D is always connected to the measurement ground ($V_D = 0$). Note that all ohmic contacts are equipped with standard RC-filters ($R = 2200\ \Omega$, $C = 2\ \text{nF}$) for noise reduction and protection from electrostatic discharge damage. Additional cable resistances ($\sim 100\ \Omega$) and capacitances ($\sim 100\ \text{pF}$) are much smaller. The resistances of the peripheral ohmic contacts are about $50\ \Omega$ and that of the inner contact $\simeq 1\ \text{k}\Omega$, all being almost independent of the magnetic field, B . This adds up to overall contact resistances of $R_i \simeq 2.4\ \text{k}\Omega$ for the peripheral contacts ($i = 1, 2, 3, 4, S, D$) and $R_A \simeq 3.4\ \text{k}\Omega$ for the inner contact. At $B = 0$, the resistance of the Hall bar itself is $R_0 \simeq 50\ \Omega$ between contacts S and D.

Contacts 1–4 serve as (electrically floating) voltage

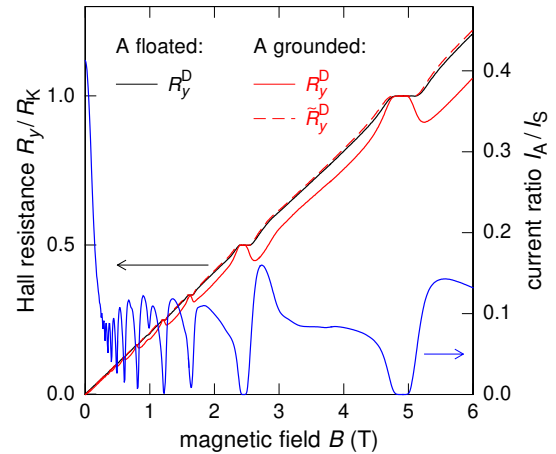


FIG. 2. Left-hand-side axis: measured Hall resistance $R_Y^D(B)$ while the inner contact is either floated (black solid line) or grounded (red solid line); the dashed red line is $\tilde{R}_Y^D(B)$, corrected for the reduced current. Right-hand-side axis: current ratio I_A/I_S while A is grounded (solid blue line).

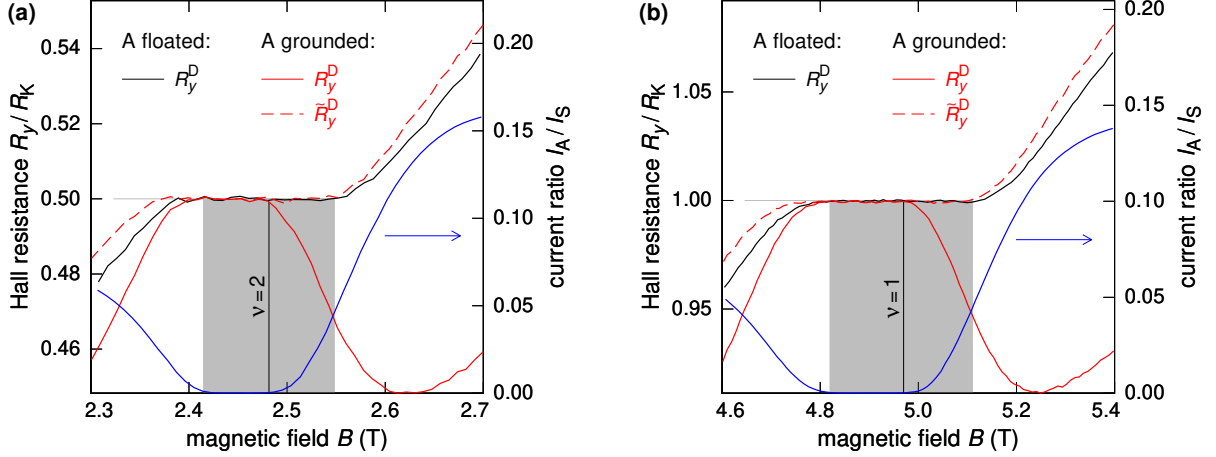


FIG. 3. Enlargements from Fig. 2 (same presentation) near filling factors $\nu = 2$ in (a) and $\nu = 1$ in (b) indicated as vertical lines. The magnetic field regions of the quantized plateaus, as determined for floating A, are depicted as gray background. On the high-field side of the integer bulk filling factor, current flows through contact A while the corrected \tilde{R}_y^D recovers the quantized plateau resistance.

probes. We simultaneously measure the four individual voltages $V_{1,2,3,4}$ in respect to ground (employing Agilent 34411A multimeters). Compared to measuring pairwise voltage differences, this increases flexibility but slightly reduces accuracy [31]. In the following, we discuss the four terminal resistances $R_{ij} = (V_j - V_i)/I_S$. They include the Hall resistances, which we relabel as $R_{14} = R_y^S$ and $R_{23} = R_y^D$ according to the voltage probe locations near the S versus D contact, and the longitudinal resistances measured along the high-potential versus low-potential edges of the Hall bar, labeled accordingly $R_{12} = R_x^{\text{high}}$ and $R_{43} = R_x^{\text{low}}$, cf. the sketch in Fig. 1(b).

If both, the drain and the inner contact, are connected to electrical ground, we deal with a three-terminal setup. To receive all three currents, we measure in addition to I_S the current flowing through the inner contact I_A using a current amplifier (Basel Precision Instruments).

III. RESULTS

If we keep the inner contact A electrically floating, its influence on the Hall effect measurements can be neglected and we find equal Hall resistances $R_y^S = R_y^D$ and correspondingly identical longitudinal resistances $R_x^{\text{low}} = R_x^{\text{high}}$, as it is expected for a homogeneous carrier density along the Hall bar. For our choice of $V_S < 0$, the source contact has an increased chemical potential and emits electrons. In respect of the flow of these electrons, the Hall resistance R_y^S is measured upstream of contact A and is identical for A being electrically floated or connected to ground. In comparison, R_y^D is measured downstream of A and, therefore, R_y^D , R_x^{high} and R_x^{low} depend on I_A , see Ref. [Supplementary Information] for a complete set of measurements.

In Fig. 2, we show the Hall resistance $R_y^D(B)$ near the drain contact (left axis) for A floated (black line) versus A connected to ground (red solid line). Connecting A to ground yields a reduction of R_y^D whenever $I_A \neq 0$; the blue line in Fig. 2 displays the current ratio $I_A(B)/I_S$ (right axis). We observe a sharp drop of $I_A(B)/I_S$ in the classical regime. For $B > 0.3$ T, it is followed by pronounced Shubnikov-de-Haas oscillations averaging to $I_A \simeq 0.08I_S$. However, I_A vanishes for the largest part of the plateaus, which indicates that the inner contact remains isolated even if grounded. To account for the current reduction downstream of A, we introduce the corrected Hall resistance $\tilde{R}_y^D = R_y^D \frac{I_S}{I_S - I_A}$, which we added in Fig. 2 as a red dashed line. At large, $\tilde{R}_y^D(B)$ recovers $R_y^D(B)$ measured with A floated. However, a detailed look reveals slight deviations and an interesting dynamics.

Focusing on the dynamics in the quantum regime in Fig. 3, we show enlarged sections of the identical data plotted in Fig. 2 covering the first two plateaus near bulk filling factors (averaged over the width of the Hall bar) $\nu = 1$ and $\nu = 2$. The shaded backgrounds indicate the plateau regions for A being floated with $R_y^D = \frac{1}{\nu}h/e^2$ and $R_x^{\text{low}} = R_x^{\text{high}} = 0$. The observed behavior is congruent for $\nu = 1$ and $\nu = 2$.

Throughout the low magnetic field side of the plateaus (for $\nu > 1$ or $\nu > 2$), the grounded inner contact is electrically isolated with $I_A = 0$ and leaves the quantized Hall plateaus unaffected, i.e., $R_y^D = R_K/\nu$. However, if we increase the magnetic field while remaining on the quantized plateau for $\nu \lesssim 1$ or $\nu \lesssim 2$, a rapidly growing fraction of the current I_S flows through the inner contact and $R_y^D < R_K/\nu$. Nevertheless, the finite $I_A \neq 0$ does not affect the quantized Hall state, since the corrected \tilde{R}_y^D exactly recovers the quantized plateau resistance.

IV. DISCUSSION

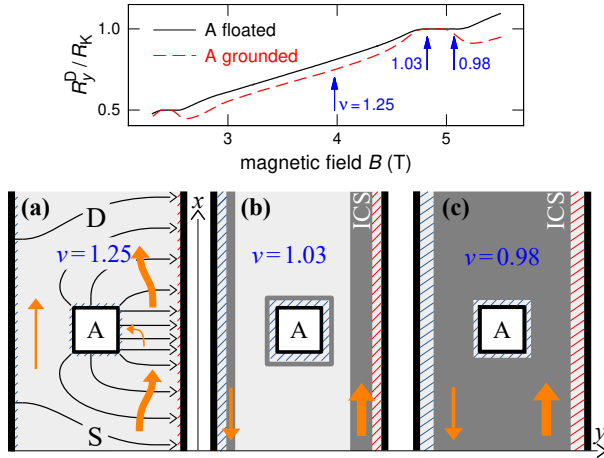


FIG. 4. **Screening theory:** Qualitative sketches of the segmentation of the Hall bar in compressible (light gray) and incompressible (dark gray) regions for contact A connected to ground at three different filling factors near $\nu = 1$ as indicated in the top panel (data from Fig. 2) for orientation. In the sketches, the insulating sample edges and a thin Schottky (tunnel) barrier around A are drawn as black lines. Areas of constant potential (always compressible) near ground are marked by blue stripes, near source (high) potential by red stripes. Orange filled arrows indicate the local flow of electrons. (a) Diffusive regime between plateaus; potential drops gradually across a compressible Hall bar; current flow is uni-directional and perpendicular to the electric field shown as thin black arrows. (b, c) Plateau region; chiral current flow restricted to ICSs; potential changes linearly inside ICSs and is constant in compressible regions; (b) features the case of edge ICSs, which in (c) widened and combined to a single bulk ICS.

Our experiments clearly demonstrate that, starting in the middle of the plateau, current flows in the bulk of the Hall bar. Even for $I_A \neq 0$, the QHE does not break down, instead we find identical plateau regions at quantized Hall resistance R_K/ν , whether the inner contact is grounded or floated, cf. Fig. 2. We interpret this finding in terms of scattering-free bulk current as follows: Whenever I_S reaches the inner contact, the drop of the chemical potential across the current carrying ICS is reduced by $e|I_A|R_K/\nu$ according to I_A branching off. This transition is adiabatic, meaning that electron scattering inside the ICS remains suppressed. Only after they left the ICS, electrons contributing to I_A start to scatter and dissipate.

While we observe $I_A \neq 0$ only on the higher-magnetic-field halves of the plateaus, the LB picture does not provide a scenario, which breaks the symmetry of the plateaus (in respect to the integer bulk filling factor). Moreover, the only way to interpret an onset of $I_A \neq 0$ based on the LB picture would be the assumption of a breakdown of the QHE induced by the grounded contact A. However, such a breakdown would be accompanied with carrier scattering and

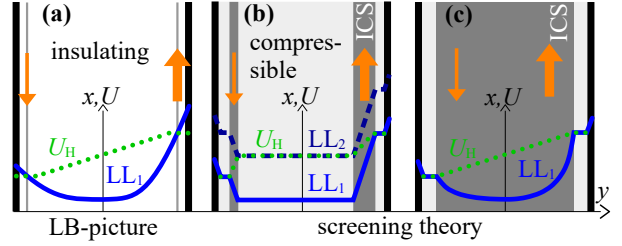


FIG. 5. Sketch of the LL energies across the Hall bar (blue lines solid for LL_1 and dashed for LL_2) and the corresponding Hall potential $U_H(y)$ (dotted green lines). LLs are completely filled at energies below $U_H(y)$, partly filled at $U_H(y)$ and empty above $U_H(y)$. (a) Situation that the LB picture assumes for the entire plateau region (white indicates insulating areas, gray lines perfect 1D edge channels). (b) and (c) Predictions of the screening theory, addressing the low- versus high-magnetic-field sides of the plateau at $\nu \simeq 1$ and corresponding to Figs. 4(b) and 4(c).

would cause a deviation from our finding $R_y^S = \tilde{R}_y^D = R_K/\nu$. We conclude, that the LB picture, although it correctly predicts the quantization of the Hall resistance, fails to describe the current density distribution across the Hall bar.

While the LB picture is a single-particle model, by considering electron-electron interactions [8, 14], the screening theory naturally explains a transition along each plateau from edge currents to scattering-free bulk current. This transition causes the asymmetry of $I_A(B)$ and $R_y^D(B)$ in respect to the integer bulk filling factor. In Fig. 4, we qualitatively sketch the prediction of the screening theory for three different filling factors. In Fig. 4(a), we show the situation for $\nu \simeq 1.25$ depicting the diffusive transport regime between plateaus (Drude model), in Fig. 4(b) and 4(c), we sketch typical situations along the quantized plateau, cf. Ref. 32 for comparable numerical calculations. In Fig. 4(b) with $\nu \simeq 1.03$, we consider the low-magnetic-field side of the plateau, where separate narrow ICSs follow along the sample edges. In Fig. 4(c) with $\nu \simeq 0.98$ at the high-field side of the plateau, a single ICS extends through the bulk of the Hall bar. Compressible regions are indicated with light gray shading, ICSs with dark gray shading. Colored striped patterns mark the compressible regions at the highest (red) and lowest (blue) potentials. In Fig. 4(a), the entire Hall bar is compressible, the Hall potential U_H drops across its entire width and current flows everywhere. The according approximate electric field distribution is drawn using thin black arrows, the current flow is indicated by thick orange arrows.

In the case of a quantized plateau as shown in Figs. 4(b) and 4(c), U_H drops entirely inside the ICSs, which are indicated using dark gray shading. We plot these Hall potentials $U_H(y)$ together with the course of the $\nu = 1$ LLs in the Figs. 5(b) and 5(c). The current flows where the potential drops, hence, for the plateaus it is restricted to the ICSs. For the case of edge ICSs, cf. Fig. 4(b), the inner contact is isolated and $I_A = 0$. However, in the diffusive regime, cf. Fig. 4(a), or if a bulk ICS exists, cf. Fig. 4(c), current can flow into contact A.

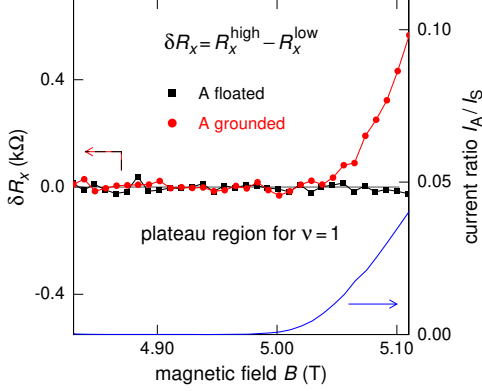


FIG. 6. Left y-axis: difference δR_x between longitudinal resistance on high versus low potential sides of the Hall bar in the region of the first plateau ($\nu = 1$) for contact A grounded (solid red line) versus A floated (dashed black line). The horizontal line indicates $\delta R_x = 0$. Right y-axis: current ratio I_A/I_S for A grounded.

The screening theory predicts that an increase of I_S results in a widening of the ICS at the high potential edge of the Hall bar (which then carries more current), cf. Figs. 4(b) and 5(b). We expect that a wider ICS (for a larger I_S) reaches the inner contact and yields $I_A \neq 0$ already at smaller B . We present measurements confirming this behavior in Sec. IV of the Ref. [Supplementary Information].

For comparison, in Fig. 5(a), we also present a sketch depicting $U_H(y)$ and the $\nu = 1$ LL as it is expected within the LB picture (uniformly for the entire plateau). In the LB picture, the bulk of the Hall bar is assumed to be insulating, such that current can flow only inside the compressible 1D edge channels. This is in clear contradiction to the prediction of the screening theory.

Finally, we discuss how the current I_A is branched off and flows into contact A for the plateau regions. For $\mu B \gg 1$ all current flows perpendicular to the local electric field direction. For $I_A = 0$, the longitudinal electric field vanishes and the perpendicular Hall field guides all current past contact A into the drain contact. In contrast, for $I_A \neq 0$ a longitudinal electric field exists along contact A and yield the longitudinal resistances $R_x^{\text{high}} > R_x^{\text{low}} > 0$. We illustrate this in Fig. 6 by plotting the difference $\delta R_x = R_x^{\text{high}} - R_x^{\text{low}}$ for the $\nu = 1$ plateau region in comparison to I_A/I_S . For contact A being floated, δR_x vanishes as expected for the plateaus, while for grounded A, δR_x becomes finite where $I_A \neq 0$. Note, that $R_x^{\text{high}} - R_x^{\text{low}} = R_y^{\text{S}} - R_y^{\text{D}}$ in accordance with Kirchhoff's voltage law, cf. Ref. [Supplementary Information]. This points to an inhomogeneous longitudinal electric field, which is larger along the high field side of contact A. It indicates, that the current I_A , too, flows into contact A mostly along its high potential side. This analysis suggests, that a longer inner contact would result in a larger I_A/I_S .

V. SUMMARY AND OUTLOOK

We have performed quantum Hall experiments using a Hall bar equipped with an inner contact, which allows us to directly measure whether current flows in the bulk of the sample. LB edge channels would bypass the inner contact, such that it remained electrically isolated. Our results indicate an asymmetry of the quantized plateaus of the Hall resistance: For the low-magnetic-field side of the plateaus (filling factor exceeding the integer value) the current through the inner contact is $I_A = 0$, suggesting that the applied current is restricted to the edges of the Hall bar. In contrast, for the high-magnetic-field side of the plateau (ν lesser than the integer value), we observe $I_A \neq 0$. Here, our results indicate the existence of scattering-free bulk current. Both, bulk current while the resistance is quantized as well as the observed asymmetry of the plateaus with scattering-free bulk current on their high-magnetic-field sides are incompatible with the LB edge channel picture. Our findings confirm the relevance of the electron-electron interactions for the dynamics in the regime of the integer QHE. Our results can be qualitatively explained within the screening theory, which includes the direct Coulomb interaction between the carriers in a semiclassical approach. A quantitative comparison would require extended numerical calculations, which is beyond the scope of this letter. In future, similar experiments in other material systems confining 2D electrons or holes would be valuable to confirm the generality of our findings.

Our result underpins the relevance of the electron-electron interaction for explaining the integer QHE, but it also suggests that we should reconsider the possible importance of the direct Coulomb interaction for other types of the QHE, including its topological variants. Moreover, the more complicated current density distribution predicted by the screening theory (compared to the LB picture) should be considered for experiments in the QHE regime, particularly for the case of phase sensitive measurements. Finally, the application of the QHE as resistant standard might be further optimized, if we manage to apply our improved microscopic understanding to create Hall bars with more stable plateaus.

ACKNOWLEDGEMENT

This work was funded by the Deutsche Forschungsgemeinschaft (DFG, German Research Foundation) – 218453298.

CONTRIBUTIONS OF THE AUTHORS

V. U. produced the sample. S. S. performed the measurements. S. S. and S. L. analyzed the data and wrote the article. A. S. contributed to the planning and provided critical feedback. S. L. led the project.

REFERENCES

- [1] K. von Klitzing, G. Dorda, and M. Pepper, New method for high-accuracy determination of the fine-structure constant based on quantized Hall resistance, *Phys. Rev. Lett.* **45**, 494 (1980).
- [2] BIPM, *Le Système international d'unités / The International System of Units ('The SI Brochure')*, ninth ed. (Bureau international des poids et mesures, 2019).
- [3] F. Delahaye and B. Jeckelmann, Revised technical guidelines for reliable dc measurements of the quantized Hall resistance, *Metrologia* **40**, 217 (2003).
- [4] Y. Ji, Y. Chung, D. Sprinzak, M. Heiblum, D. Mahalu, and H. Shtrikman, An electronic Mach-Zehnder interferometer, *Nature* **422**, 415–418 (2003).
- [5] V. J. Goldman and B. Su, Resonant tunneling in the quantum Hall regime: Measurement of fractional charge, *Science* **267**, 1010–1012 (1995), <https://www.science.org/doi/pdf/10.1126/science.267.5200.1010>.
- [6] M. Büttiker, Four-terminal phase-coherent conductance, *Phys. Rev. Lett.* **57**, 1761 (1986).
- [7] M. Büttiker, Absence of backscattering in the quantum Hall effect in multiprobe conductors, *Phys. Rev. B* **38**, 9375 (1988).
- [8] D. B. Chklovskii, B. I. Shklovskii, and L. I. Glazman, Electrostatics of edge channels, *Phys. Rev. B* **46**, 4026 (1992).
- [9] D. B. Chklovskii, K. A. Matveev, and B. I. Shklovskii, Ballistic conductance of interacting electrons in the quantum Hall regime, *Phys. Rev. B* **47**, 12605 (1993).
- [10] M. M. Fogler and B. I. Shklovskii, Resistance of a long wire in the quantum Hall regime, *Phys. Rev. B* **50**, 1656 (1994).
- [11] K. Lier and R. R. Gerhardt, Self-consistent calculations of edge channels in laterally confined two-dimensional electron systems, *Phys. Rev. B* **50**, 7757 (1994).
- [12] A. Siddiki and R. R. Gerhardt, Thomas-fermi-poisson theory of screening for laterally confined and unconfined two-dimensional electron systems in strong magnetic fields, *Phys. Rev. B* **68**, 125315 (2003).
- [13] A. Siddiki and R. R. Gerhardt, Incompressible strips in dissipative Hall bars as origin of quantized Hall plateaus, *Phys. Rev. B* **70**, 195335 (2004).
- [14] R. R. Gerhardt, The effect of screening on current distribution and conductance quantisation in narrow quantum Hall systems, *physica status solidi (b)* **245**, 378 (2008), <https://onlinelibrary.wiley.com/doi/pdf/10.1002/pssb.200743344>.
- [15] P. Armagnat and X. Waintal, Reconciling edge states with compressible stripes in a ballistic mesoscopic conductor, *Journal of Physics: Materials* **3**, 02LT01 (2020).
- [16] We note, that we disagree with a recent suggestion of the current flowing along the interfaces between ICSSs and compressible regions, based on applying the continuity equation at equilibrium [15]. However, even if this suggestion was correct, it would not change the interpretation of our experiment, that we find a transition from edge to bulk current along the plateaus of quantized Hall resistance.
- [17] K. Güven and R. R. Gerhardt, Self-consistent local equilibrium model for density profile and distribution of dissipative currents in a hall bar under strong magnetic fields, *Phys. Rev. B* **67**, 115327 (2003).
- [18] I. Kaya, G. Nachtwei, B. Sagol, K. von Klitzing, and K. Eberl, Spatial evolution of the generation and relaxation of excited carriers near the breakdown of the quantum Hall effect, *Physica E: Low-dimensional Systems and Nanostructures* **6**, 128–131 (2000).
- [19] V. Yu, M. Hilke, P. J. Poole, S. Studenikin, and D. G. Austing, Phase diagram of quantum hall breakdown and nonlinear phenomena for InGaAs/InP quantum wells, *Phys. Rev. B* **98**, 165434 (2018).
- [20] P. Haremski, M. Mausser, A. Gauß, K. von Klitzing, and J. Weis, Electrically induced breakdown of the quantum Hall effect at different Hall bar widths: Visualizing the edge- and bulk-dominated regimes within a quantum Hall plateau, *Phys. Rev. B* **102**, 205306 (2020).
- [21] A. Siddiki and R. R. Gerhardt, Range-dependent disorder effects on the plateau-widths calculated within the screening theory of the iqhe, *International Journal of Modern Physics B* **21**, 1362 (2007), <https://doi.org/10.1142/S0217979207042847>.
- [22] K. L. McCormick, M. T. Woodside, M. Huang, M. Wu, P. L. McEuen, C. Duruo, and J. S. Harris, Scanned potential microscopy of edge and bulk currents in the quantum Hall regime, *Phys. Rev. B* **59**, 4654 (1999).
- [23] P. Weitz, E. Ahlswede, J. Weis, K. Klitzing, and K. Eberl, Hall-potential investigations under quantum Hall conditions using scanning force microscopy, *Physica E: Low-dimensional Systems and Nanostructures* **6**, 247 (2000).
- [24] J. Horas, A. Siddiki, J. Moser, W. Wegscheider, and S. Ludwig, Investigations on unconventional aspects in the quantum hall regime of narrow gate defined channels, *Physica E: Low-dimensional Systems and Nanostructures* **40**, 1130 (2008), 17th International Conference on Electronic Properties of Two-Dimensional Systems.
- [25] A. Siddiki, J. Horas, J. Moser, W. Wegscheider, and S. Ludwig, Interaction-mediated asymmetries of the quantized hall effect, *EPL (Europhysics Letters)* **88**, 17007 (2009).
- [26] A. Siddiki, J. Horas, D. Kupidura, W. Wegscheider, and S. Ludwig, Asymmetric nonlinear response of the quantized hall effect, *New Journal of Physics* **12**, 113011 (2010).
- [27] J. Weis and K. von Klitzing, Metrology and microscopic picture of the integer quantum Hall effect, *Philosophical Transactions of the Royal Society A: Mathematical, Physical and Engineering Sciences* **369**, 3954 (2011), <https://royalsocietypublishing.org/doi/pdf/10.1098/rsta.2011.0198>.
- [28] Kendirlik E. M., Sirt S., Kalkan S. B., Dietsche W., Wegscheider W., Ludwig S., and Siddiki A., Anomalous resistance overshoot in the integer quantum Hall effect, *Scientific Reports* **3**, 3133 (2013).
- [29] E. M. Kendirlik, S. Sirt, S. B. Kalkan, N. Ofek, V. Umansky, and A. Siddiki, The local nature of incompressibility of quantum Hall effect, *Nature Communications* **8**, 14082 (2017).
- [30] G. M. Ferguson, R. Xiao, A. R. Richardella, D. Low, N. Samarth, and K. C. Nowack, Direct visualization of electronic transport in a quantum anomalous hall insulator, *Nature Materials* **22**, 1100–1105 (2023).
- [31] To explore the highest possible accuracy of our multimeters we calibrated them using the measured Hall resistances of the

- quantized plateaus. The corrections are $< 1\%$.
- [32] A. Yildiz, D. Eksi, and A. Siddiki, The consequences of bulk compressibility on the magneto-transport properties within the quantized Hall state, *Journal of the Physical Society of Japan* **83**, 014704 (2014), <https://doi.org/10.7566/JPSJ.83.014704>.

Supplementary information: Direct measurement of bulk currents in the quantized Hall regime

S. Sirt,¹ V. Y. Umansky,² A. Siddiki,³ and S. Ludwig^{1,*}

¹Paul-Drude-Institut für Festkörperelektronik, Leibniz-Institut im Forschungsverbund Berlin e.V., Hausvogteiplatz 5-7, 10117 Berlin, Germany

²Weizmann Institute of Science, 234 Herzl Street, POB 26, Rehovot 76100, Israel

³Istanbul Atlas University, Hamidiye, Anadolu Cd. no:40, 34408, Istanbul, Turkey

I. COMPLETE SET OF HALL MEASUREMENTS

In Fig. S1, we sketched the sample including a simplified

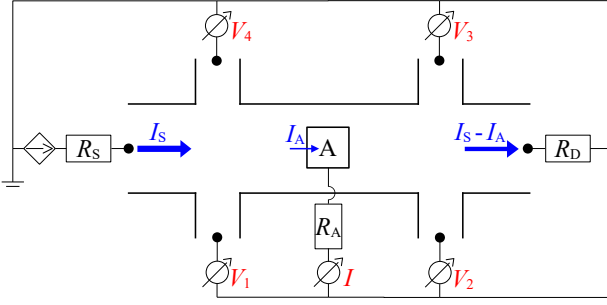


FIG. S1. Sketch of the sample with a simplified circuit diagram of the set-up. The current I_S is applied (and measured) using a constant current source. I_A flowing via the contact resistance R_A to ground is measured as well, if contact A is grounded. The remainder of the current flows via the contact resistance R_D to ground. The voltage probes 1–4 are kept electrically floating, while the voltages $V_{1,2,3,4}$ are simultaneously measured with four separate multimeters.

circuit diagram of our measurement set-up. In Fig. S2, we plot both, Hall and longitudinal resistances as a function of B , while the inner contact A is electrically floated [panel (a)] in comparison to the case when A is connected to ground [panel (b)]. While A is floated, we find the expected relations $R_y^S = R_y^D$ and $R_x^{\text{high}} = R_x^{\text{low}}$, suggesting that our inner contacts do not alter the Hall effect while floated [1]. If we ground the inner contact, R_y^S remains unchanged but we observe $R_y^D \leq R_y^S$ and $R_x^{\text{low}} \leq R_x^{\text{high}}$. The potential differences of a closed loop sum up to zero and, accordingly, we expect $R_y^S - R_y^D = R_x^{\text{high}} - R_x^{\text{low}}$. This is experimentally confirmed in Fig. S3, suggesting that the four individual voltmeters are correctly calibrated. Note that we compared the quantized Hall resistances at the plateaus with the von-Klitzing constant in order to control and, if necessary, fine-tune the calibration of the voltmeters. In the diffusive limit, the longitudinal voltage drop difference $R_x^{\text{low}} < R_x^{\text{high}}$ indicates that, while the inner contact is grounded, the current density is reduced on the low-potential side of the Hall bar and accordingly increased on its high-potential side. It confirms our sketch in Fig. 4(a) of the main article.

II. DEPENDENCE OF THE BULK CURRENT ON THE APPLIED CURRENT I_S AND BREAKDOWN

The electrically induced breakdown of the QHE [2, 3], i.e., its dependence on the applied voltage was studied in Ref. 4 for various Hall bar widths. The authors reported that the breakdown depends on the width of the Hall bar at the high magnetic field ends of the plateaus while they found a much smaller width dependence at the low magnetic field ends of the plateaus. These findings support the screening theory predictions of bulk (edge) transport at the high (low) magnetic field ends of the plateaus: the observed breakdown behavior suggests that edge transport is independent of the Hall bar width while bulk transport depends on the width.

Here, we study the electrically induced breakdown as a function of the current applied through the source contact I_S . At the same time, we explore the dependence of the current flowing through the grounded inner contact I_A on I_S . In Fig. S4, we present the Hall resistance $R_y^D(B) = \frac{V_2 - V_3}{I_S}$, its corrected value $\tilde{R}_y^D(B) = \frac{V_2 - V_3}{I_S - I_A}$ and the current through the inner contact $I_A(B)$ for various values of the applied current I_S , which is increased from top to bottom. We consider the filling factors near $\nu = 2$ in Fig. S4(a) versus $\nu = 1$ in Fig. S4(b). Areas shaded in gray approximately indicate the magnetic field regions of the plateau of the corrected Hall resistance, $\tilde{R}_y^D = R_K/\nu$. The decrease of this gray area as I_S is increased indicates the electrically induced breakdown of the QHE. The breakdown happens on both ends of the plateau with subtle variations related with edge versus bulk transport at the two ends of the plateau [4].

In Fig. S4 we also indicate as a blue stripe pattern the magnetic field regions of $I_A = 0$ (coinciding with $R_y^D = R_K/\nu$ and integer ν). On the low magnetic field side the onset of $\tilde{R}_y^D < R_K/\nu$ coincides with the onsets of $I_A \neq 0$ and $R_y^D < R_K/\nu$ (with integer $\nu = 1, 2$). The behavior is quite different at the high magnetic field side of the plateau. As discussed in the main article the onset of $I_A \neq 0$ with $R_y^D < R_K/\nu$ do not coincide with the onset of $\tilde{R}_y^D > R_K/\nu$. The reason is the bulk current presented by I_A , which flows through the Hall bar. As we increase I_S the onset of $I_A \neq 0$ shifts to smaller B independently of and more rapidly than the breakdown induced decrease of the plateau width (gray areas). This finding indicates, that the magnetic field region of scattering-free bulk current increases with growing I_S .

This behavior is indeed predicted by the screening theory: Starting from the low magnetic field side of the plateau we consider two ICSs, one along each edge. A higher current I_S increases the width of the ICS near the high potential edge of

* sirt@pdi-berlin.de; ludwig@pdi-berlin.de

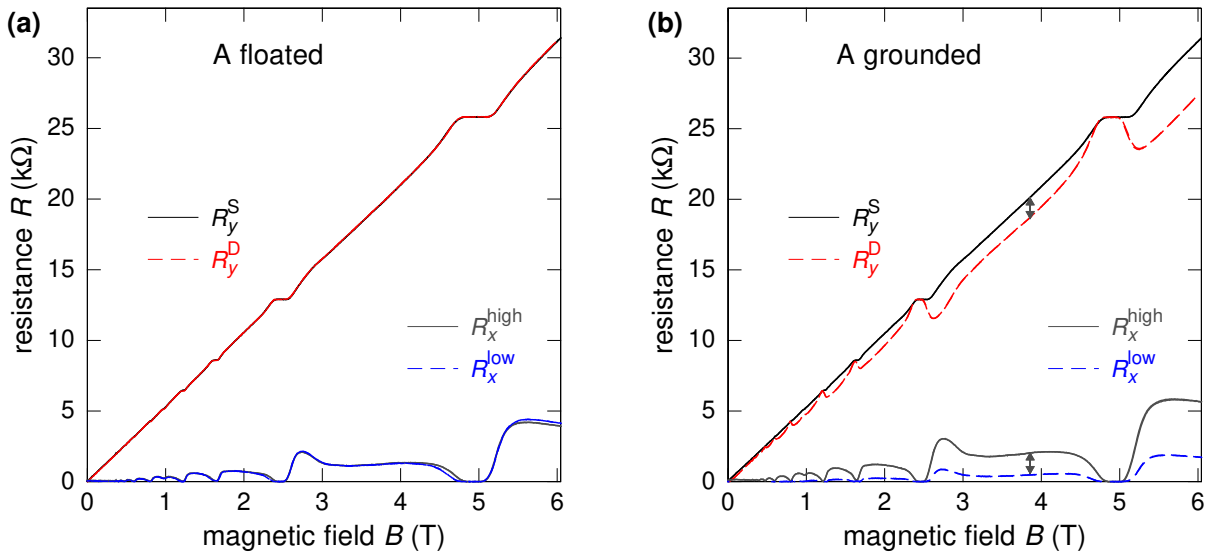


FIG. S2. Hall resistances R_y and longitudinal resistances R_x while the inner contact A is kept electrically floated (a) or connected to ground (b). The two grey double arrows in (b) have identical length.

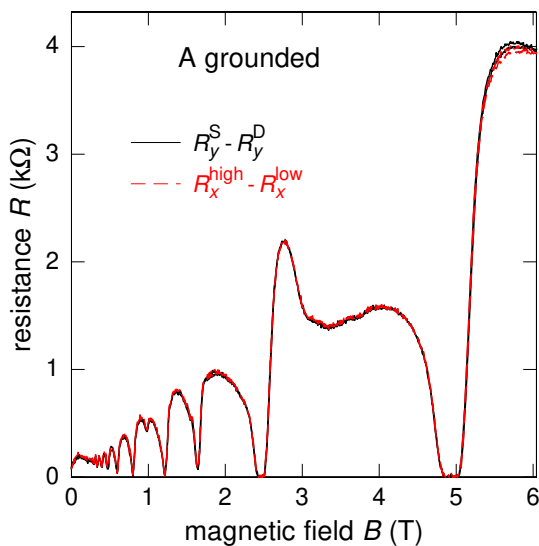


FIG. S3. The inner contact A is connected to ground. The difference between the Hall resistances matches the difference between the longitudinal resistances. After multiplying the resistances with I_S , this confirms Kirchhoff's voltage law stating that the direct sum of potential differences around a closed loop is zero.

the Hall bar as it has to carry more current (e.g., see Figure 9 in Ref. 5). The wider ICS naturally fosters the transition from edge to bulk transport, such that $I_A \neq 0$ starts at smaller values of B .

In summary, our I_S dependent measurements qualitatively confirm the predictions of the screening theory for the current

dependence of the transition from edge to bulk transport.

III. CURRENT THROUGH THE INNER CONTACT

In Fig. S5, we present the measured inner current I_A (μB) as in Fig. 2 of the main article. If we also consider the enlargements shown in Fig. 3 of the main article, we observe four different regimes in regard to the current I_A that flows through the inner contact.

- i. *Scattering-free edge current*: within the lower-magnetic-field regions of the plateaus, the entire current flows without scattering along the edges of the Hall bar such that the inner contact is completely isolated and $I_A = 0$, cf. Fig. 3 of the main article.
- ii. *Scattering-free bulk current*: within the higher-magnetic-field regions of the plateaus, the current still flows without scattering but spreads through the bulk of the Hall bar. A fraction of the current flows through the inner contact, cf. Fig. 3 of the main article.
- iii. *Classical regime for $B < 0.3\text{T}$* : at $B = 0$, about 42 % of I_S flows through the inner contact related with the ratio of the contact resistances $R_D \simeq 2.4\text{k}\Omega$ and $R_A \simeq 3.4\text{k}\Omega$. As the magnetic field is increased, I_A/I_S drops to about 8 % in average.
- iv. *Diffusive regime for $B > 0.3\text{T}$* : the Landau quantization causes an oscillation of I_A/I_S around the average value of about 8 %. This oscillation includes the regions of quantized Hall plateaus, regimes i. and ii. above. It also includes regions of diffusive current between the Hall plateaus shaping the local maxima of I_A .

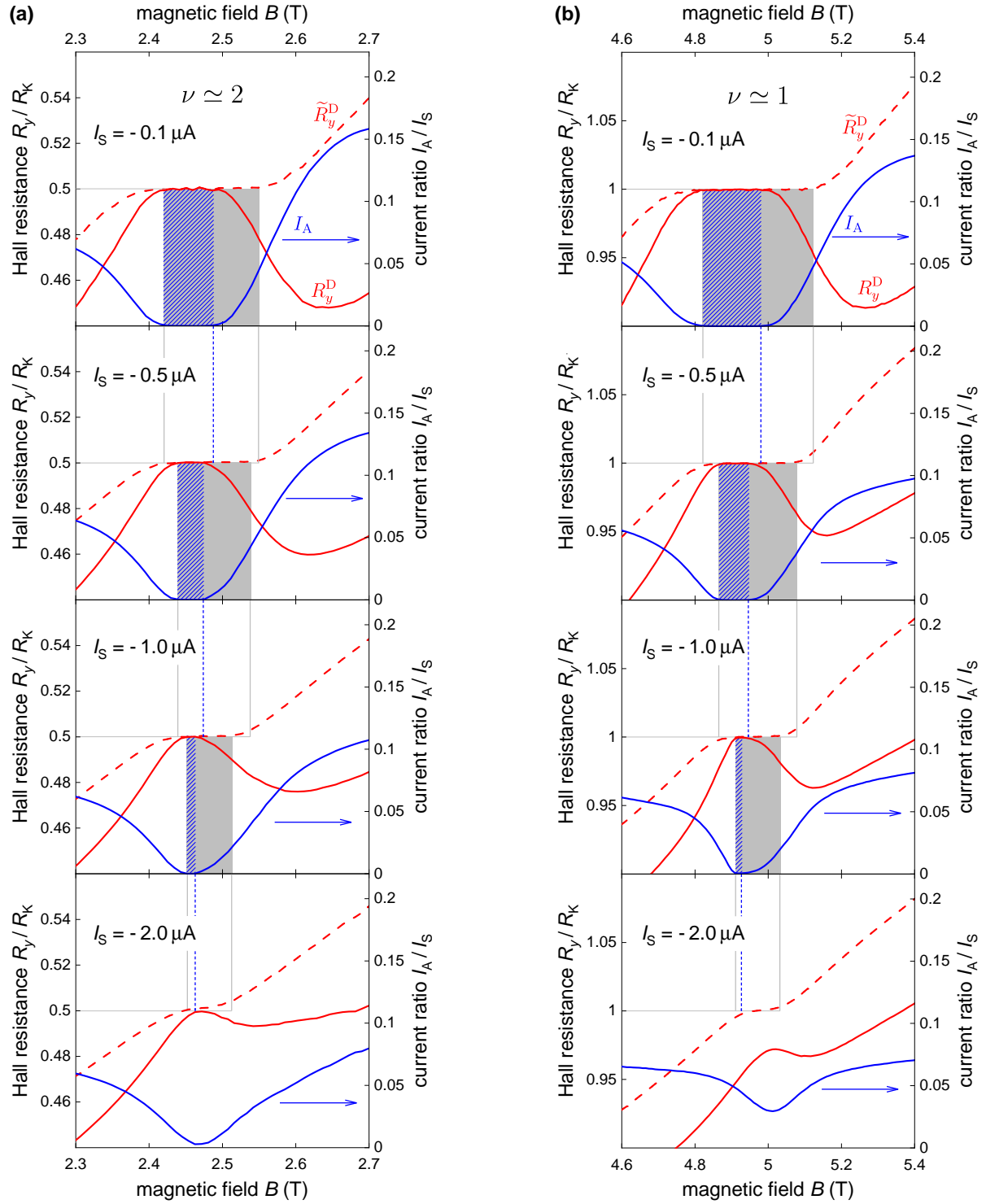


FIG. S4. Hall resistances $R_y^D(B)$ (red-solid) and $\tilde{R}_y^D(B)$ (red-dashed) as well as the current ratio $I_A/I_S(B)$ (blue solid line, right hand side axes) for filling factors $\nu \approx 2$ in (a) and $\nu \approx 1$ in (b). From top to bottom, the current I_A applied through the source contact is increased. The inner contact A is connected to ground. The gray areas indicate the plateau region with $R_y^D = R_K/\nu$ and $\nu = 1, 2$. The blue patterned areas indicate magnetic field regions with $I_A = 0$ and $R_y^D = R_K/\nu$.

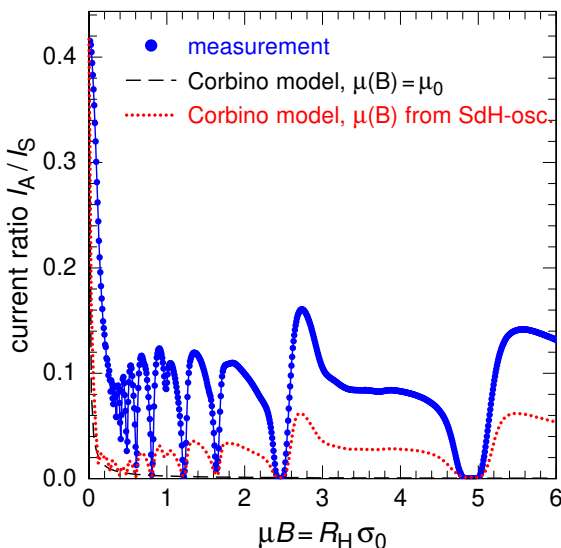


FIG. S5. Ratio of the currents flowing through the inner contact and the source contact I_A/I_S as a function of B . The dashed black and red dotted lines are model curves assuming a Corbino geometry, cf. main text, for a constant mobility $\mu_0 = \mu(B=0) = 396 \text{ m}^2/\text{Vs}$ or the strongly oscillating $\mu(B)$ determined from the longitudinal resistance measurements with the inner contact floated, respectively.

In Fig. S5 we compare $I_A(B)/I_S$ with a classical prediction assuming a Corbino geometry centered around the inner contact, $I_A(B)/I_S = \sqrt{(I_A(0)/I_S)^2 + (\mu B)^2/[1 + (\mu B)^2]}$. In this model we assumed that for $\mu B \gg 1$ the Hall voltage between the Hall-bar edge and the inner contact drives I_A , and we interpolate between this model for $\mu B \gg 1$ and the value of $I_A(0)/I_S$ actually measured at $B = 0$. The dashed black line is the model prediction, if we assume a constant mobility $\mu_0 = \mu(B=0) = 396 \text{ m}^2/\text{Vs}$. However, in reality, $\mu(B)$ strongly oscillates related with the Shubnicov-de-Haas oscillations of the longitudinal resistance. The red dotted line in Fig. S5 shows our model prediction using the oscillating $\mu(B)$ determined from the measured longitudinal resistance $R_x(B)$, while the inner contact was floated. For all magnetic fields $B > 0$ with $I_A(B)/I_S \neq 0$ our actually measured current ratio $I_A(B)/I_S$ substantially exceeds the prediction. Clearly, the two-terminal Corbino model does not correctly describe our three-terminal experiment.

To better understand the difference between the Corbino disk geometry and our three-terminal setup, we consider the longitudinal voltage drop, namely $V_1 - V_2 \simeq R_H I_A$, which exists because of the grounded drain contact and which is located across the inner contact and along the high-potential edge of the Hall bar. Corresponding to a longitudinal electric field (along the inner contact), in the presence of the perpendicular magnetic field, $V_1 - V_2$ bends excess current into contact A. Clearly, an elongated inner contact would result in a larger I_A/I_S , respectively, $V_1 - V_2$.

IV. DIFFUSIVE LIMIT OF THE CORRECTED HALL RESISTANCE

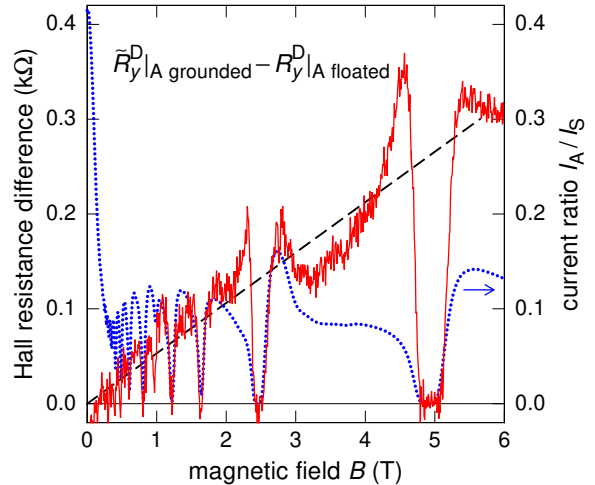


FIG. S6. Difference between the Hall resistances with contact A grounded versus A floated, $\tilde{R}_y^D|_{A \text{ grounded}} - R_y^D|_{A \text{ floated}}$, as a function of B (solid red line) and the current $I_A(B)$ flowing through A (dotted line, right-hand-side axis). The black dashed line in the background is proportional to B .

The corrected Hall resistance $\tilde{R}_y^D = R_y^D \frac{I_S}{I_S - I_A} = \frac{V_2 - V_3}{I_S - I_A}$ accounts for the reduced current flowing downstream of the inner contact A. In the diffusive regime (away from the quantized plateaus) we find that \tilde{R}_y^D with $I_A \neq 0$ slightly exceeds $R_H = \frac{B}{en}$. In Fig. S6, we plot $\tilde{R}_y^D|_{A \text{ grounded}} - R_y^D|_{A \text{ floated}}$ in order to visualize this excess Hall resistance. At its local maxima, I_A approximately increases proportional to B and accounts for $\sim 1\%$ of R_y^D . We conjecture that the excess Hall resistance for grounded A is another feature of the self-consistent steady-state solution which also explains I_A . In a nut shell, the voltage drop $V_1 - V_2$ corresponds to a charge density drop along the high-potential edge of the Hall bar. Charge diffusion along the edge then causes an increase of $|V_2|$, which is proportional to R_H , and an according increase of $\tilde{R}_y^D = \frac{V_2 - V_3}{I_S - I_A}$ (note that $|V_3| \simeq 0$).

Another contribution to the observed excess Hall voltage might be a reduced effective carrier density n_s beyond the grounded inner contact. This would be related to the inhomogenous current distribution across the Hall-bar caused by the grounded inner contact. In particular, an enhanced current near the high-potential edge of the Hall bar, where $n_s(y)$ decreases, yields a decreased average n_s . A quantitative prediction of both discussed effects would require elaborate numerical calculations which go beyond the scope of this article.

REFERENCES

-
- [1] Tiny deviations in the measurement (beyond statistical noise) are caused by a slightly imperfect calibration of the four separate voltmeters.
- [2] I. Kaya, G. Nachtwei, B. Sagol, K. von Klitzing, and K. Eberl, Spatial evolution of the generation and relaxation of excited carriers near the breakdown of the quantum Hall effect, *Physica E: Low-dimensional Systems and Nanostructures* **6**, 128–131 (2000).
- [3] V. Yu, M. Hilke, P. J. Poole, S. Studenikin, and D. G. Austing, Phase diagram of quantum hall breakdown and nonlinear phenomena for InGaAs/InP quantum wells, *Phys. Rev. B* **98**, 165434 (2018).
- [4] P. Haremski, M. Mausser, A. Gauß, K. von Klitzing, and J. Weis, Electrically induced breakdown of the quantum Hall effect at different Hall bar widths: Visualizing the edge- and bulk-dominated regimes within a quantum Hall plateau, *Phys. Rev. B* **102**, 205306 (2020).
- [5] R. R. Gerhardt, The effect of screening on current distribution and conductance quantisation in narrow quantum Hall systems, *physica status solidi (b)* **245**, 378 (2008), <https://onlinelibrary.wiley.com/doi/pdf/10.1002/pssb.200743344>.